The University of Michigan HIPLATE Experiment

W. Sanders*, D. R. Dowling*, M. Perlin, S. L. Ceccio***

***Mechanical Engineering**
****Naval Architecture and Marine Engineering**

University of Michigan
Ann Arbor, MI 48109

Abstract: Our group at the University of Michigan is currently conducting an experimental program to examine friction drag reduction at large size scales and high Reynolds numbers. We will be examining polymer and microbubble friction drag reduction as it occurs in a near-zero pressure gradient boundary layer. The program, designated the HIPLATE experiment, is described.

Introduction: Renewed interest in high-speed ocean transport by the Defense Department of the United States has led to a number of new drag reduction research programs. Emphasis has been placed on friction drag reduction through the injection of gas or polymers into turbulent boundary layers. Research has been focused on the multi-scale aspects of these flows, with experiments and numerical simulations being conducted over a range of Reynolds numbers. Our group at the University of Michigan is contributing to this overall effort with the experimental examination of friction drag reduction at high Reynolds numbers and large size scales. We are beginning with the examination of the near-zero-pressure gradient boundary layer that forms over a flat plate at high Reynolds numbers – the "HIPLATE" experiment.

The skin friction produced by a turbulent boundary layer can be reduced by as much as 80% with the introduction of polymers or bubbles into the boundary layer in laboratory scale flows with Reynolds numbers (based on downstream distance) to several million (see, for example, McCormick and Bhattacharya, 1973; Merkle and Deutsch, 1993 for microbubble injection and Toms, 1948; Berman, 1978; Escudier et al., 1999, and Choi, 2000 for polymer drag reduction). Because of the potential benefits for improved efficiency of water-craft of all kinds, literally thousands of articles on this subject have appeared in the last thirty or forty years. Yet, the basic mechanisms underlying skin-friction reduction remain unresolved, especially for the case of microbubble-turbulence interactions.

At a more practical level, the promise of 80% drag reduction is of great interest to the designers and operators of ocean transportation systems, particularly if vessel speed or fuel consumption is important. However, few of the skin-friction or drag reduction experiments to date (in the unclassified literature) have addressed the critical issue of how to scale the various skin-friction reduction schemes and approaches examined in the laboratory. These methods must achieve the same percentage drag reduction at Reynolds numbers typical of full-scale ocean-going vessels (10^9 to 10^{10}).

The HIPLATE experiment addresses both the science and scaling issues through a series of controlled but large-scale experiments involving a large test model placed in the world's largest water tunnel, the U. S. Navy's William B. Morgan Large Cavitation Channel (LCC). Unique insight into the physical phenomena leading to drag reduction will be obtained through extensive measurements within thick (boundary layer thickness of order 10 cm) high-Reynolds number boundary layers (2×10^8 based on downstream length) with and without to presence of polymers, air bubbles, or both. This size scale allows precision measurements with modern non-intrusive optical diagnostics and enhances the relative resolution of flush-mounted wall sensors.

This paper will present an outline of the HIPLATE experiments, the suite of experimental measurements, and describe the on-going test program.

William B. Morgan Large Cavitation Channel (LCC): Figure 1 shows a picture and a schematic of the LCC, located in Memphis, Tennessee. The LCC is operated by the Naval Surface Warfare Center. It is a recirculating water tunnel with a nominal test section length of 13 meters and cross section of 3m × 3m. The LCC may be repeatably operated at water flow speeds from 0.5 to 18.3 m/s.

Figure 1a. The US Navy's Large Cavitation Channel. The LCC is the world's largest water flow facility. Note the size of the people at the left and right edges of this picture.

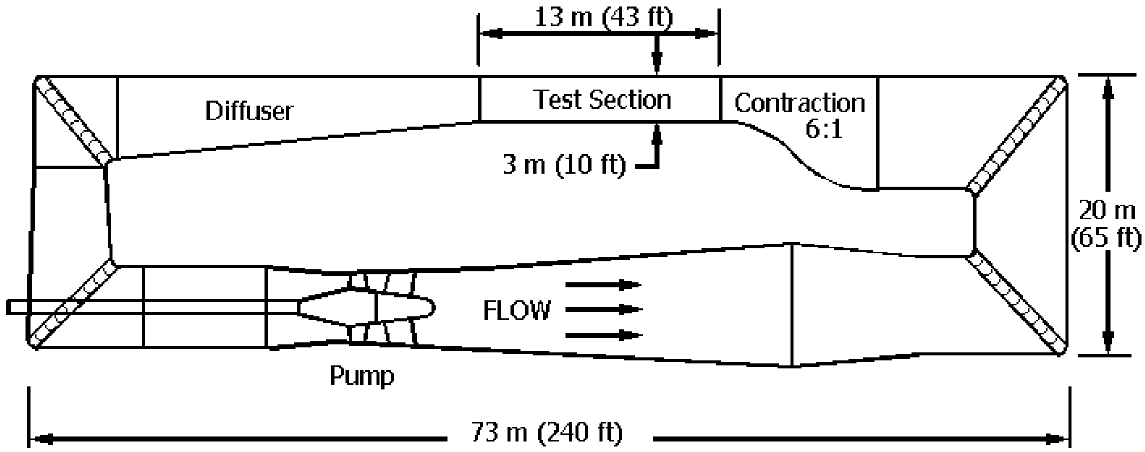

Figure 1b. Schematic of the US Navy's Large Cavitation Channel. The maximum flow speed in the test section is slightly above 18 m/s. The maximum Reynolds number based on the test section length is greater than 200 million.

The HIPLATE Test Model: We will be conducting large-scale controlled tests to examine in detail the process of polymer and microbubble drag reduction at high Reynolds numbers and large scales (Figure 2). We will first examine the turbulent boundary layer flow over a flat, hydraulically smooth surface. This geometry, while simple, has several advantages. First, the flow over the flat surface is well understood, and it should be possible to readily discern the effects of polymer or bubble addition. Second, many lab-scale tests have been performed with this geometry, and our test model can be used to aid in Reynolds number scaling as it will be the largest ever tested. Third, this geometry can be used to explore the buoyancy effects associated with micro-bubble injection (using “plate-up” and “plate-down” injection configurations by flipping the model).

Figure 3 shows the engineering drawing of the HIPLATE. The model is composed of the three plate sections. Each is composed of a mild-steel, welded frame, with stainless-steel outer skin. The three plates are mounted together with an interlocking set of keys and slots, and each plate is independently mounted at four points using rectangular tangs. The leading edge of the plate is a 4:1 ellipse, and the trailing edge is a truncated wedge. The plate was fully assembled, and the instrumentation side finish machined to create a smooth and undisrupted flat surface. The surface roughness of the instrumentation side is 10-20 μin.

The instrumentation side of the plate has been equipped with multiple penetrations for flush mounted instrumentation and line injection into the boundary layer. The model has been designed to be mountable upside-down for to examine the effect of buoyancy. There are three main measurement stations on the model. This number is dictated by the optical access to the model through the windows of the LCC. The instrumented side will be reversed to study the influence of bubble buoyancy. A wide variety of instrumentation will be used. Interchangeable plates will be used on the diagnostic surface so that the instruments may be rearranged, removed, or replaced.

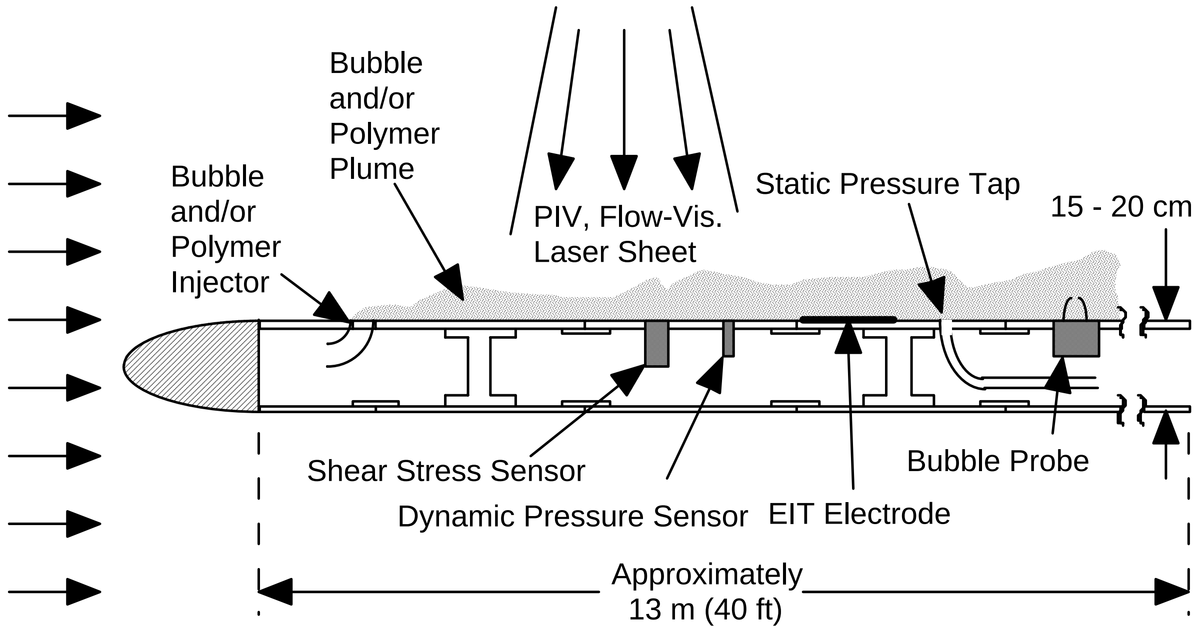

Figure 2. Schematic diagram of the drag reduction test model.

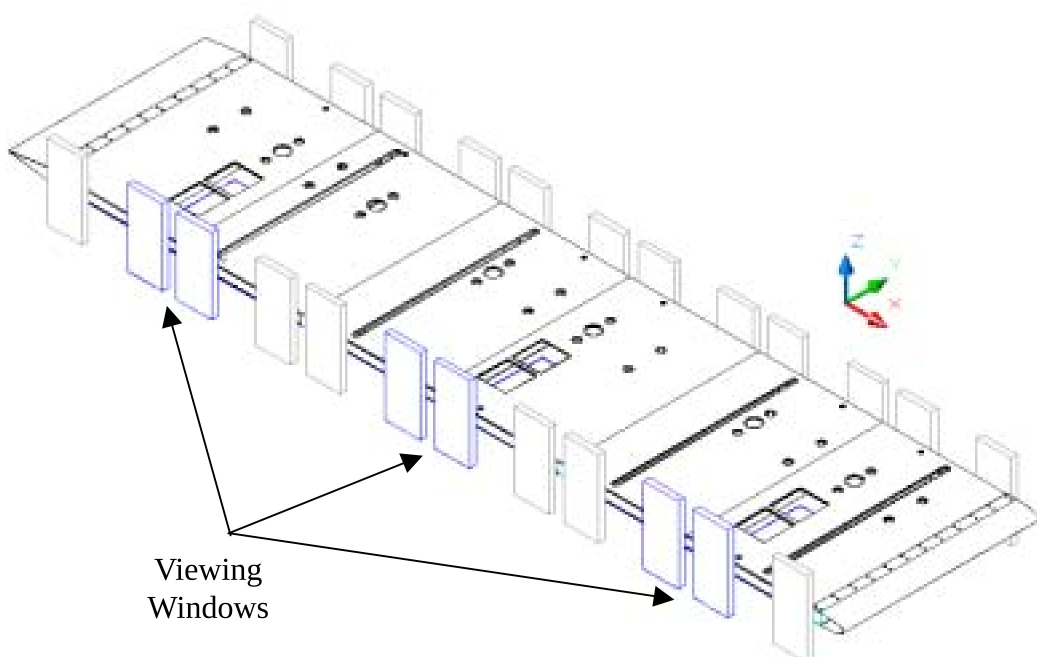

Figure 3: Engineering drawing of the HIPLATE model as it fits into the LCC test section.

The Experimental Suite: A variety of instruments will be used to examine the turbulent boundary layer as it develops over the HIPLATE. The location of each instrument along the HIPLATE model is depicted in Figure 4.

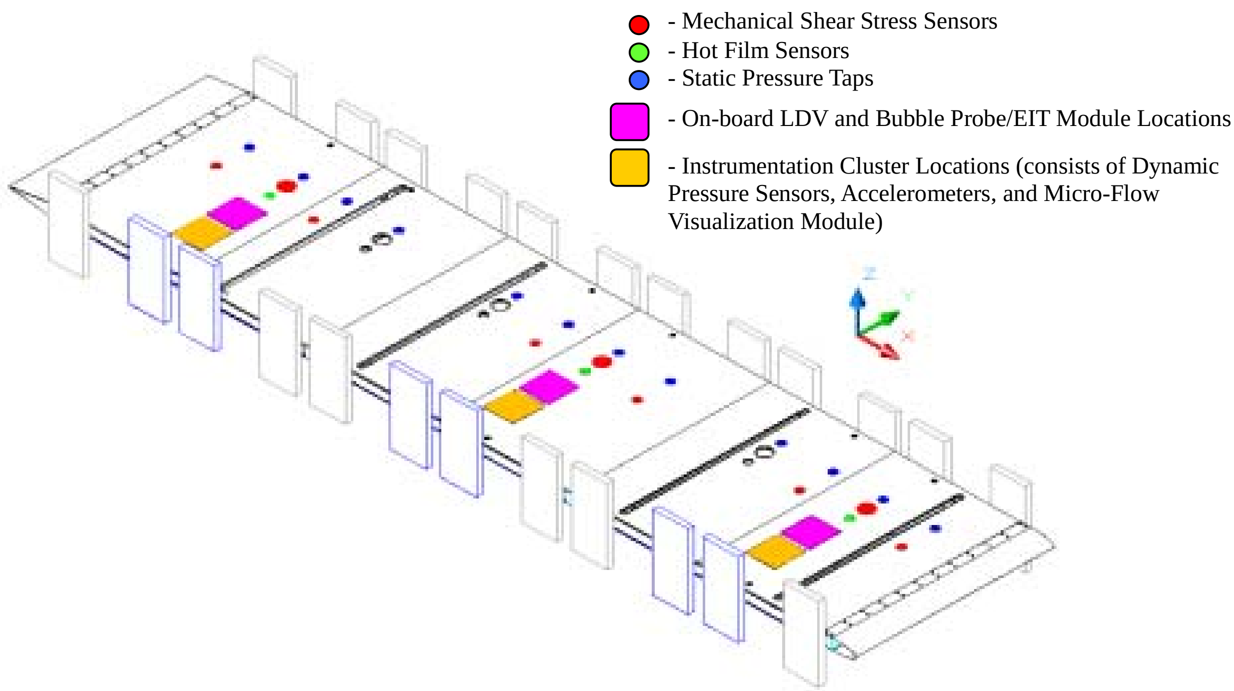

Figure 4: Instrumentation lay-out on the HIPLATE model.

Static Surface Pressure Measurements: We will be able to measure pressures at 48 or more locations on the model and test section. These will be used to set the pressure gradient along the turbulent boundary layer. We will measure both the pressures along the turbulent boundary layer and along the test section walls. The latter measurement is important to establish boundary conditions for numerical models of the flow.

Average Skin Friction Measurements: Unlike usual laboratory experiments, we will not measure the integrated drag force on the entire model. However, because the model is large, we can measure the integrated skin friction over large areas of the boundary layer using a “floating plate” supported on strain-gage balances. These sensors are manufactured by Sankei Engineering of Japan. This type of sensor will provide the most robust measure of the skin friction reduction**.** Two different sized sensors (six with a diameter of 10mm and three with a diameter of 100mm) are used for these friction drag measurements. The large sensors are located in the same streamwise location as all of the other diagnostics, and the smaller sensors are located just upstream and downstream of each large sensor. They are flush-mounted with the surface of the model to ensure accurate wall friction measurement. As these sensors are mechanical (not optical), they will be the crucial diagnostic in assessing the level of friction drag reduction during both polymer and microbubble injection.

Local Dynamic Skin Friction Measurements: Three flush-mounted hot-film anemometers manufactured by TSI, Inc. will be used to examine the local variation in skin friction. These measurements are important to determine the nature of the turbulent flow near the wall. The hot film sensors will function in tandem with the mechanical shear stress sensors, where the average shear stress measurements will provide the nominal value for the dynamic measurements. Such probes will work well for both the natural and polymer injected flows. However, care must be taken when using them for bubbly flow measurements.

Local Surface Pressure Fluctuation: Flush-mounted dynamic pressure transducers manufactured by PCB Piezotronics, Inc. will be used to examine the pressure fluctuations near the locations of the skin friction sensors. These measurements are also important to determine the nature of the turbulent flow near the wall. We will be able to simultaneously measure fluctuating pressure with sixteen sensors forming an L-array with streamwise dimension of 0.264 m and cross-stream dimension of 0.391 m. These sensors will provide spatial and temporal correlation functions, as well as auto- and cross-spectra.

Accelerometers: One-dimensional accelerometers manufactured by Wilcoxin Research will be used to examine the local vertical vibration of the model at six locations. This is both a safety measure as well as a vibrational diagnostic to assist in detecting flow patterns that are a result of a forced vibration in the model.

On-Board LDV: This optical diagnostic is manufactured by VioSense, Inc. and is a one-component miniature Laser Doppler Velocimetry module. It fits entirely into the model so that it is capable of resolving near-wall mean and fluctuating velocity components. It has an in-water probe length 60 μm in the cross-stream and 20 μm in the streamwise direction. There are three potential measuring stations, all of which are co-located with the rest of the diagnostics.

Planar Particle Imaging Velocimetry (PIV): PIV will be used to examine the flow within the turbulent boundary layer. The use of PIV for the investigation of turbulent flows is now well established (Adrian, 1991). The advantages and limitations of PIV on the laboratory scale are known. Conducting PIV measurement in the LCC presents some unique challenges, but a system has been developed for use in the LCC as part of the large hydrofoil experiment (the HIFOIL experiment) conducted in 2001 (Bourgoyne et al. 2001). We have implemented a double-pulsed planar PIV system capable of capturing two double-pulsed images at a rate of 4 Hz. The interrogation region would be on the order of 0.1 m by 0.1 m or much less. The resolution of the PIV system is sufficient to resolve a wide range of scales within the high-Reynolds number turbulent boundary layer. PIV data will be taken at the same three locations as the On-Board LDV and the major instrumentation clusters (see Figure 4) to ensure continuity in the different measurements. The PIV system cannot be used to examine the flow within the bubbly boundary layer, however.

Laser Doppler Velocimetry (LDV): The LCC is equipped with two LDV systems. One is used to monitor the freestream conditions, and the second can be used to measure two or three components of the flow over the model. This system will be used to augment the PIV measurements, and the LDV data acquisition will be performed at the same streamwise locations as the PIV data acquisition. The LDV system cannot be used to examine the flow within the bubbly boundary layer.

Micro-Flow Visualization: This diagnostic will be used for visualizing the turbulent flow near the surface of the plate. It has the capability of using dye injection, PIV particles and streak visualization as potential methods of viewing the flow. It uses a Sony XC-55B camera with remote head and a shutter speed range of 1/4 - 1/100,000 seconds. It also uses a Bitflow frame-grabber and Video Savant frame recorder. The camera can be moved small distances from a remote-access translation stage, and the shutter speeds are controlled from outside of the test section. The overall goal is to examine the flow from $0 < y+ < 100$.

Local Bubble Probes: Local conductivity probes have been developed to measure both the local void fraction and average bubble size in dense bubbly flows. Ceccio and George (1996) provide a review of these designs and applications. Conductivity probes are problematic in that they are intrusive, they will not work for very small bubbles, and they require substantial calibration. However, they are the only robust method to determine average bubble sizes. For the present tests, bubbles probes will be designed that can accurately determine both the bubble mean sizes and local void fractions for flows with speeds in excess of 10 m/s over as wide a range of bubble sizes as possible.

Electrical Impedance Tomography (EIT): EIT is a novel technology that can be used to measure the distribution of void fraction without *in-situ* placement of probes in the multiphase flow. Electrical currents are injected at the boundary of the domain and resulting voltages are recorded. These boundary data are used to solve an ill-posed inverse problem, then reconstruct the distribution of electrical impedance within the domain. If the phases of a multiphase flow have significantly different electrical impedances (such as air and water), the mixture impedance can be used to infer the local void fraction. A description of these systems can be found in George and Ceccio (1996). Prof. Ceccio has been working with the Department of Energy's Sandia National Laboratory (SNL) in Albuquerque, NM, to develop these systems for high void-fraction gas—liquid flows. Such a system was developed and used to measure the high void-fraction gas-holdup in a bubble column (George *et al.*, 2000). Prof. Ceccio continues to work with researchers at SNL to expand the use of EIT for gas—liquid flows, and he currently has support from the National Science Foundation to develop these systems for solid-gas flows. An EIT system is proposed for the current project to determine the distribution of void fraction within the bubbly mixture of the boundary layer. The spatial resolution of the EIT system is insufficient to resolve individual bubbles; however, the temporal resolution of the EIT system may be sufficient to reveal large-scale time-variations of the gas density *within* the bubbly boundary layer.

High Speed Cinematography: We will use high-speed digital cinematography to record the dynamics of the bubbly turbulent boundary layer. A Kodak digital imaging system is available that can image to 2000 frames per second with high resolution and to 40,000 frames per second with reduced resolution. This system will be used to examine the dynamics of the bubbly mixture. A second Kodak system with intensified imager and one-half full-frame imaging rates at less resolution is also available.

Test Conditions: With the HIPLATE installed in the LCC, we are able to achieve the range of test conditions shown in Figure 5.

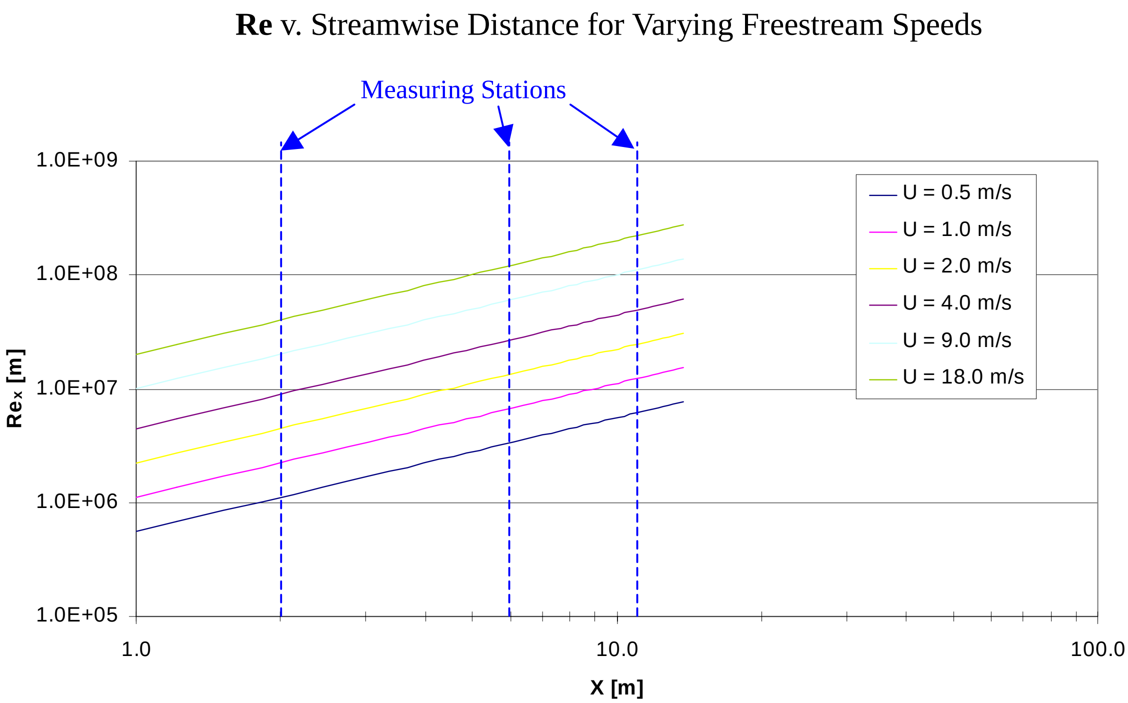

Figure 5: Range of Reynolds numbers examined in the HIPLATE experiment. Tripping will be used near the leading edge to stimulate boundary layer transition.

Measuring stations are located at 2.0m, 5.9m, and 10.7m downstream from the leading edge, which allows us to examine a range of Reynolds numbers (based on downstream distance) from one million to 200 million. This range achieves higher Reynolds numbers than any previously performed flat plate boundary layer experiment, but also spans a wide enough range that the lowest Reynolds numbers examined in our experiment will overlap with previous experimental results.

Phase 1 Testing and Current Status: The HIPLATE was fabricated over the summer and fall of 2001, and it was installed in the LCC during November and December of 2001 for “shake-down” testing. Figures 6a and 6b show the HIPLATE mounted in the LCC. No polymer of bubble injection was implemented in Phase 1. Instead, the un-tripped boundary layer of the model was examined. Phase 1 was also used to assess and improve the instrumentation suite.

Figure 6a: HIPLATE model (as seen from the tail section looking upstream) mounted in the LCC.

Figure 6b: Polished nose section (4:1 ellipse) of the HIPLATE model as seen mounted in the LCC.

We are currently working with our sponsors to plan the next phase of HIPLATE testing. Current discussions suggest a round of both microbubble injection testing and a series of "polymer ocean" experiments. We expect that these tests will conducted in June 2002.

Acknowledgements: We would like to acknowledge the support of the U.S. Defense Advanced Research Project Agency (DARPA) (Dr. L. J. Porter, Dr. P. Albright, and Capt. J. Kamp, monitor), the U. S. Office of Naval Research (ONR) (Dr. L. P. Purtell, monitor), the Naval Surface Warfare Center – Carderock Division (R. Etter and D. Schwarzenberg), J & J Burning and Lincoln Park Boring (model fabricators), and the University of Michigan (Dwayne Bourgoyne, Josh Hamel, Kent Pruss and Warren Eaton).

References:

Adrian, R. (1991) *Ann. Rev. Fluid Mech.,* Vol. 23, 261-304.

Berman, N. (1978) *Ann. Rev. Fluid Mech.,* Vol. 10, 47-64.

Bourgoyne, D., S. L. Ceccio, D. R. Dowling, S. Jessup, J. Park, W. Brewer, and R. Pankajakshan, (2000) *Proc. 23rd Symp. On Naval Hydrodynamics,* Val de Reuil, France.

Ceccio, S. L. and D. L. George, (1996) *J. Fluids Engrg.*, Vol. 118, 391-399.

Choi, K.-S. (2000) *Fluid Dynamics Research*, Vol. 26, 325-335.

Escudier, M. P., F. Presti, S. Smith, (1999) *J. of Non-Newtonian Fluid Mech.,* Vol. 81, 197-213.

George, D. L., J. R. Torczynski, K. A. Shollenberger, T. J. O'Hern, and S. L. Ceccio, (2000) *Int. J. of Multiphase Flow*, Vol. 26, 549-581.

McCormick, M. and Bhattacharya (1973) *Naval Eng. J.,* Vol. 85, 11-16.

Merkle, C. and Deutsch, S. (1993) *Appl. Mech. Rev*., Vol. 45, 103-127.

Toms, B. A. (1948) *Proc. 1st. Int. Congr. Rheol*., Vol. 2, 135-41.